Influence of the Lipid Anchor Motif of N-Ras on the Interaction with Lipid Membranes: A Surface Plasmon Resonance Study

Andrea Gohlke,[†] Gemma Triola,[‡§] Herbert Waldmann,[‡§] and Roland Winter[†*]
[†]Faculty of Chemistry, Physical Chemistry I—Biophysical Chemistry and [‡]Department of Chemistry, Chemical Biology, Technische Universität Dortmund, Dortmund, Germany; and [§]Max Planck Institute of Molecular Physiology, Department of Chemical Biology, Dortmund, Germany

ABSTRACT Ras GTPases play a crucial role in signal transduction cascades involved in cell differentiation and proliferation, and membrane binding is essential for their proper function. To determine the influence of the nature of the lipid anchor motif and the difference between the active (GTP) and inactive (GDP) forms of N-Ras on partitioning and localization in the lipid membrane, five different N-Ras constructs with different lipid anchors and nucleotide loading (Far/Far (GDP), HD/Far (GDP), HD/HD (GDP), Far (GDP), and HD/Far (GppNHp)) were synthesized. Using the surface plasmon resonance technique, we were able to follow the insertion and dissociation process of the lipidated proteins into and out of model membranes consisting of pure liquid-ordered (l_o) or liquid-disordered (l_d) phase and a heterogeneous two-phase mixture, i.e., a raft mixture with $l_o + l_d$ phase coexistence. In addition, we examined the influence of negatively charged headgroups and stored curvature elastic stress on the binding properties of the lipidated N-Ras proteins. In most cases, significant differences were found for the various anchor motifs. In general, N-Ras proteins insert preferentially into a fluidlike, rather than a rigid, ordered lipid bilayer environment. Electrostatic interactions with lipid headgroups or stored curvature elastic stress of the membrane seem to have no drastic effect on the binding and dissociation processes of the lipidated proteins. The monofarnesylated N-Ras exhibits generally the highest association rate and fastest dissociation process in fluidlike membranes. Double lipidation, especially including farnesylation, of the protein leads to drastically reduced initial binding rates but strong final association. The change in the nucleotide loading of the natural N-Ras HD/Far induces a slightly different binding and dissociation kinetics, as well as stability of association, and seems to influence the tendency to segregate laterally in the membrane plane. The GDP-bound inactive form of N-Ras with an HD/Far anchor shows stronger membrane association, which might be due to a more pronounced tendency to self-assemble in the membrane matrix than is seen with the active GTP-bound form.

INTRODUCTION

The rat-adeno-sarcoma (Ras) GTPases act as molecular switches cycling between an active GTP-bound and an inactive GDP-bound state and regulate the signal cascades initiated by cell surface receptors to control processes like cell differentiation, proliferation, and apoptosis (1). Deregulation by mutation of these proteins is found in ~30% of all human cancers (2,3). The Ras family consists of three isoforms, namely H (Harvey)-, N (neuroblastoma)-, and K (Kirsten)-Ras. The structures of the protein cores of these isoforms are almost identical, but low sequence similarity is observed at the C-terminus, which may explain the different functions of these proteins (4). Ras proteins are post-translationally modified in different ways via lipidation at their C-terminal hypervariable region (HVR). All isoforms comprise a common C-terminal S-farnesyl (Far) cysteine methylester. In the case of H-Ras, N-Ras (Fig. 1), and K(A)-Ras, stable membrane association is achieved by double lipidation, which confers a hydrophobic stretch essential for membrane binding and function. Next to an S-farnesyl thioether of these proteins, one or two cysteine residues are present, and these residues undergo reversible S-palmitoylation at cysteine SH-groups. In contrast, K(B)-Ras comprises a polybasic region of six lysines (3,5), which together with the farnesyl moiety confers association with the membrane. To act as regulators of signaling pathways, these proteins are activated upon nucleotide exchange from the GDP- to the GTP-bound form. Upon depalmitoylation, N-Ras traffics back to the Golgi apparatus or gets ubiquitinated and subsequently degraded (6,7). It is believed that the lipidation itself, as well as the composition of the membrane, influences the protein function and its intramembrane distribution, as well as the interaction with effectors. In particular, the formation of membrane subdomains or nanoclusters, but also other properties of the membrane, for example, charges, can play an important role in the partitioning and function of membrane-associated proteins (8–17). Studies on model systems suggest, in addition, that the preferred binding sites may be not the membrane domains themselves, but rather the interface between two phases (18).

To understand protein-membrane interactions in detail, generally the roles of a series of physical and chemical parameters have to be considered. In the context of signal transduction, the interaction involves recruitment of the protein at the cell membranes, which often involves electrostatic and hydrophobic interactions as well as protein-protein interactions or clustering of the embedded proteins. Furthermore, cholesterol-containing microdomains or so-called lipid rafts may play an important role in signal transduction (17,19).

Submitted October 2, 2009, and accepted for publication February 2, 2010.

*Correspondence: roland.winter@tu-dortmund.de

Editor: Hagan Bayley.

0006-3495/10/05/2226/10 $2.00

doi: 10.1016/j.bpj.2010.02.005

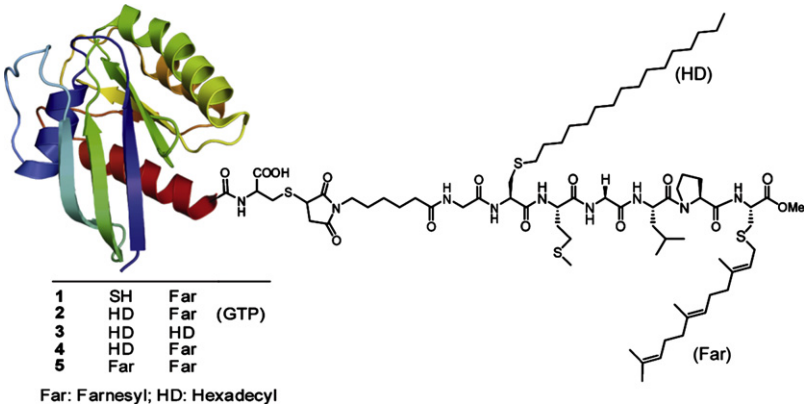

FIGURE 1 Schematic of the semisynthetic N-Ras with the different anchor systems and nucleotides investigated (SH, unmodified; HD, hexadecyl; Far, Farnesyl). If no nucleotide is mentioned, the protein is in the inactive, GDP-bound state.

Although the binding behavior of N-Ras has been studied by NMR (20,21), atomic force microscopy (AFM) (18), fluorescence microscopy (22), and infrared reflection absorption spectroscopy (23), the binding constants and the kinetics of the binding process of the N-Ras lipoprotein to a bilayer, as well as the role of the lipid anchor systems in this process, have not been addressed yet to our knowledge. To yield detailed insight into the interaction of the lipidated Ras proteins with the membrane and the influence of membrane composition on binding, we used surface plasmon resonance (SPR) to study the kinetics of binding, i.e., the association and dissociation properties, of N-Ras comprising different kinds of lipid anchor systems (Far, HD/HD, HD/Far, and Far/Far, in their GDP-bound form, as well as the active state HD/Far GTP) (Fig. 1) to various model biomembranes. In these semisynthetic proteins, the labile S-palmitoyl thioesters are replaced by stable hexadecyl thioethers (HD). The SPR technique allows real-time measurement of biomolecular binding to biomimetic surfaces without the application of a specific label, as the method depends only on a change of the refractive index (i.e., the angle of resonance), which means a change in adsorbed mass at the sensor surface. The influence of liquid-ordered (l_o) and liquid-disordered (l_d) domains, as well as their coexistence (raft mixtures), and also the influence of negative charges and stored curvature elastic stress of the membrane on the binding properties were determined.

MATERIALS AND METHODS

Materials

Lipids (1,2-dioleoyl-*sn*-glycero-3-phosphocholine (DOPC) (100%), 1,2-dipalmitoyl-*sn*-glycero-3-phosphocholine (DPPC) (100%), 1,2-dioleoyl-*sn*-glycero-3-(phospho-rac-(1-glycerol)) (sodium salt) (DOPG) (100%), and 1,2-dioleoyl-*sn*-glycero-3-phosphoethanolamine (DOPE) (100%)) were purchased from Avanti Polar Lipids (Alabaster, AL), and cholesterol (Chol) (≥99%) was obtained from Sigma Aldrich (Deisenhofen, Germany). HEPES (≥99.5%), octyl β-D-glucopyranoside, guanidine hydrochloride (≥99%), and 3-((3-cholamidopropyl)-dimethylammonio)-1-propanesulfonate (CHAPS) (≥98%) were purchased from Sigma Aldrich, and bovine serum albumin (BSA) was from Pierce (Bonn, Germany). The extruder and suitable polycarbonate membranes (0.1 μM) and filter supports were purchased from Avanti Polar Lipids, and larger membrane filters (0.2 μM), as well as the pioneer L1 sensor chip, were obtained from GE Healthcare (Munich, Germany).

Six different N-Ras constructs with different lipid anchors and nucleotide loading (Far/Far (GDP), HD/Far (GDP), HD/HD (GDP), Stbut/Far (GDP), HD/Far (GppNHp, 5′-guanosyl-(β,γ-imido)-triphosphate)), and nonlipidated N-Ras (GDP)) were synthesized as previously described (24–30). In brief, the semisynthetic N-Ras proteins were synthesized from N-Ras peptides embodying the lipid anchors and the HVR and equipped with an *N*-terminal maleimide group via a combination of solid and solution-phase strategies using F-moc-4-hydrazinbenzoyl NovaGel or 2-chlorotrityl resin. These peptides were coupled to a bacterially expressed truncated N-Ras protein carrying a cysteine at the C-terminus. As the cysteine 181 SH is the only surface-accessible group, this group was conjugated to the maleimido group of the peptide (24). Nucelotide exchange was performed as described in previous studies (31,32).

Methods

Liposome formation

At first, lipid stock solutions were prepared in chloroform and mixed at the desired molar composition of DOPC, DPPC/Chol (7:3), DOPC/DPPC/Chol (1:2:1), DOPC/DOPG (7:3), and DOPC/DOPE (7:3). The majority of the chloroform was evaporated in a gaseous nitrogen stream and afterward dried overnight under vacuum to remove the remaining solvent and then stored at −20°C. Before the experiments, the lipids were resuspended in 1 mL 10 mM HEPES buffer (pH 7.4) with 5 mM $MgCl_2$ and vortexed to yield a concentration of 3 mM. After hydration, the lipid solution was sonicated for 15 min at 40°C (65°C for the DPPC-containing mixtures) followed by five freeze-thaw-vortex cycles and another brief sonication. Large unilamellar vesicles (LUVs) were formed by extrusion through a polycarbonate filter with a 100-nm pore diameter. This common procedure is used to yield reproducible LUVs of definite size (33). The extruded solution was then diluted to a concentration of 0.5 mM.

SPR experiments

SPR experiments were carried out with a Biacore 3000 system (Biacore, Uppsala, Sweden). SPR detects binding of molecules to a surface by measuring changes in the resonance angle (34). The resonance angle depends on the refractive index above the surface, thus allowing time-dependent measurements of biomolecular adsorption to a surface. The resulting sensorgram comprises a plot of the SPR signal in resonance units (RU; 1 RU = 1 pg mm^{-2}) against time. The RU unit is a common way to present SPR data, referring to the surface coverage with protein in terms of mass protein/mm^2 surface area. The vesicle capture (L1) sensor chip was introduced for analysis of model membrane systems by SPR. It is composed of a thin dextran matrix modified by lipophilic compounds on a gold surface,

where the lipid bilayer system can be prepared through the capture of liposomes by the lipophilic compounds. The chip has been shown to be suitable for the generation of model membrane systems that provide a flexible lipid bilayer surface that closely resembles the surface of a cellular membrane (34,35). All measurements were carried out at a temperature of 25°C, whereas samples were cooled at 13°C in the autosampler before the measurement was started.

The running buffer contained 10 mM HEPES and 5 mM $MgCl_2$, pH 7.4. The L1 chip was docked, primed four times with running buffer, then washed with a cleaning program injecting 20 μL of 2-propanol/50 mM NaOH (2:3), 3 M guanidine hydrochloride, and 40 mM octyl β-D-glucopyranoside at a flow rate of 10 μL/min. Then, 15 μL of the LUVs were passed over the surface twice at a flow rate of 2 μL/min and afterward stabilized by 50 μL of buffer at a flow rate of 100 μL/min and three 10-μL injections of 25 mM NaOH at a flow rate of 5 μL/min. For every lipid mixture, a separate flow cell was used. Finally, after baseline stabilization, samples of 150 μL of N-Ras diluted in running buffer to a concentration as indicated, were injected at a flow rate of 100 μL/min to reduce rebinding and the effect of mass transfer limitation. The dissociation phase was recorded for 30 min. Thereafter, the chip was regenerated using the cleaning program until all adsorbate was washed away and the resonance signal decreased to the baseline level, sometimes including 20 mM CHAPS if usual cleaning was not efficient enough. After this procedure, a new experiment could be conducted. All solutions were filtered in advance through a 0.2-μm-pore filter and degassed. All sensorgrams were recorded at a frequency of 10 Hz. The degree of coverage of lipids on the chip was determined by the use of 0.5 μM BSA and was found to be in all studies at least 80% (typically well above 90%). To eliminate the binding effect of the pure buffer and the effect of nonspecific binding of the protein to the pure L1 chip, depending on the measured coverage as determined by BSA, these (small) signals were subtracted from the actual sensorgrams of the respective injected protein solutions. For evaluation, the baseline before injection of the respective protein was set to zero.

The fact that we could not detect saturation during injection of N-Ras HD/Far GDP, even after prolonging the injection time or increasing the protein concentration, indicates that the association of N-Ras to lipid bilayers is a rather slow and intricate process. The procedure for fitting the SPR data was selected on the basis of a multistep model of protein-membrane interactions, which involves initial (e.g., electrostatic) interactions followed by insertion/dissociation of the protein into/out of the hydrophobic interior of the membrane, as well as reorientation and potential clustering of the proteins, which has been observed experimentally by AFM for some of the N-Ras proteins (18).

The model used describes two reaction steps that, in terms of protein-lipid interactions, correspond to

$$\mathrm{P} + \mathrm{L} \underset{k_{\mathrm{off},1}}{\overset{k_{\mathrm{on},1}}{\rightleftharpoons}} \mathrm{PL} \underset{k_{\mathrm{off},2}}{\overset{k_{\mathrm{on},2}}{\rightleftharpoons}} \mathrm{PL}^*, \qquad \text{(Scheme 1)}$$

where peptide (P) in the solution binds to lipids (L) in the immobilized bilayer; PL represents the primary binding site and PL* a secondary peptide-lipid complex (e.g., representing clustering) after relocation of protein and lipid molecules within the lipid bilayer plane; $k_{\mathrm{on},1}$, $k_{\mathrm{on},2}$, $k_{\mathrm{off},1}$, and $k_{\mathrm{off},2}$ represent the association and dissociation rates of the respective parts of the reaction. In addition, a term for limitation of mass transfer in the SPR experiment, expressed by the parameter k_t, was added, which takes into account that at surfaces with high binding capacity, the binding rate may be limited by diffusion. Equations 2 and 3 are the kinetic equations. The initial concentrations $c = c(t)$ at time $t = 0$ in the bulk and at the lipid interface, respectively, are

$$\begin{aligned} c_{\mathrm{P}}(\mathrm{bulk}) &= c_{\mathrm{P}}^0,\ c_{\mathrm{P}}(0) = 0,\ c_{\mathrm{L}}(0) = R_{\max},\ c_{\mathrm{PL}}(0) \\ &= 0,\ c_{\mathrm{PL}^*}(0) = 0, \end{aligned} \qquad (2)$$

where $R_{\max}$ expresses the maximum binding capacity of the immobilized lipid membrane.

$$\begin{aligned} -\frac{dc_{\mathrm{P}}}{dt} &= k_{\mathrm{on},1} \times c_{\mathrm{P}} \times c_{\mathrm{L}} - k_{\mathrm{off},1} \times c_{\mathrm{PL}} - k_t\left(c_{\mathrm{p}}^0 - c_{\mathrm{P}}\right) \\ \frac{dc_{\mathrm{L}}}{dt} &= -\left(k_{\mathrm{on},1} \times c_{\mathrm{P}} \times c_{\mathrm{L}} - k_{\mathrm{off},1} \times c_{\mathrm{PL}}\right) \\ \frac{dc_{\mathrm{PL}}}{dt} &= k_{\mathrm{on},1} \times c_{\mathrm{P}} \times c_{\mathrm{L}} - k_{\mathrm{off},1} \times c_{\mathrm{PL}} - k_{\mathrm{on},2} \\ &\quad \times c_{\mathrm{PL}} + k_{\mathrm{off},2} \times c_{\mathrm{PL}^*} \\ \frac{dc_{\mathrm{PL}^*}}{dt} &= k_{\mathrm{on},2} \times c_{\mathrm{PL}} - k_{\mathrm{off},2} \times c_{\mathrm{PL}^*}. \end{aligned} \qquad (3)$$

The response signal R (in RU) is proportional to the amount of protein immobilized in the lipid bilayer (c_{PL}, c_{PL^*}), based on the difference of sample and running buffer. Curve fitting was performed using the Marquardt-Levenberg algorithm. The fitted curves were generated by numerical integration of the differential equations that describe the reaction scheme (Eq. 3). This fitting procedure was implemented in the BIAevaluation software 4.1 (Biacore, Uppsala, Sweden).

Owing to this complex reaction scheme, the maximum error bars of the fits were sometimes quite high due to error propagation. Hence, we fitted the association and dissociation parts of the sensorgrams also separately. The initial association process (for $t \to 0$), which is directly proportional to $k_{\mathrm{on},1}$, was determined by linear regression using BIAevaluation software 4.1, and the dissociation phase was also fitted to a biexponential model (see Eq. 4) using Origin 7 (OriginLab, Northampton, MA), which yields information about two independent dissociation constants (e.g., from a loosely bound and a clustered state) and their respective contributions A_1 and A_2,

$$R = A_1 \times \mathrm{e}^{-k_{\mathrm{off},1}(t-t_0)} + A_2 \times \mathrm{e}^{-k_{\mathrm{off},2}(t-t_0)} + \mathrm{offset} \qquad (4)$$

(where t_0 is the time point at which the flow cell switched to pure buffer solution), and allows calculation of an average dissociation rate constant $\overline{k}_{\mathrm{diss}}$:

$$\overline{k}_{\mathrm{diss}} = \frac{A_1}{A_1 + A_2} \times k_{\mathrm{off},1} + \frac{A_2}{A_1 + A_2} \times k_{\mathrm{off},2}. \qquad (5)$$

The relative amount of quasi-irreversibly bound protein was derived by correlating the offset of the biexponential fit to the initial amplitude at the starting point ($t = 0$) of the dissociation phase.

The error bars in all experiments represent the standard deviation from at least three (up to six) independently conducted experiments. To test the results also with a view to their significance, we conducted a one-sided two-sample t-test using Origin 7 software. The prespecified significance level was set to 5%. The p-values given in the text represent the probabilities of obtaining test statistics at least as extreme as the one that was actually observed, assuming that the null hypothesis is true, i.e., that there is no difference between the two data distributions. p-values smaller than the signifance level indicate significant differences between the two data distributions.

RESULTS

The aim of this study was to investigate the influence of combinations of lipid anchors of N-Ras on the association and dissociation behavior in various model membranes using the SPR technique. We investigated four different combinations of lipid anchor systems. On one side, monofarnesylated N-Ras and doubly lipidated N-Ras HD/Far in its inactive (GDP-loaded) or active form (with GppNHp, a nonhydrolyzable analog of GTP) were synthesized. These proteins resemble the naturally occurring N-Ras proteins in cells.

On the other side, with the aim of studying the contribution of each lipid moiety, other N-Ras proteins bearing unnatural lipid combinations were also synthesized (i.e., doubly hexadecylated (HD/HD) or doubly farnesylated (Far/Far)) (Fig. 1). The HD residue was chosen as a nonhydrolyzable, and therefore more stable, analog of the naturally occurring palmitoyl residue. As a control, we measured the binding of nonlipidated protein to the membrane as well.

We prepared membranes with different characteristics, consisting of pure l_d (DOPC) or l_o (DPPC/Chol (7:3, molar)) phase, as well as a heterogeneous two-phase mixture (DOPC/DPPC/Chol (1:2:1, molar)), i.e., a raft mixture with $l_d + l_o$ phase coexistence (36,37). In addition, we examined the influence of negatively charged headgroups (DOPC/DOPG, (7:3, molar)) and stored curvature elastic stress (DOPC/DOPE, (7:3, molar)) of the lipid bilayer on the binding properties of the lipidated N-Ras proteins.

It may be expected that the binding (and dissociation) of membrane-active signaling proteins occurs via at least a two-step process, including initial binding of the protein by electrostatic or hydrophobic interaction and embedding of the lipid anchor(s) into the hydrocarbon region of the lipid bilayer or particular domains thereof. Moreover, the lipidated protein may relocate on the lipid surface at domain interfaces and cluster via (membrane-mediated) protein-protein interactions. Hence, the association and dissociation phases of all proteins were investigated and analyzed assuming a two-step process, as described above (Scheme 1). An example of the primary data and the results of the fitting procedure is given in Fig. 2. As can be clearly seen, the SPR sensorgrams for the different anchor systems of the lipidated N-Ras protein in fluidlike (l_d) DOPC bilayers exhibit marked differences owing to their different association and dissociation rates. We evaluated quantitatively the two apparent k_{on} and k_{off} values defined in Eq. 3. In addition, the association and dissociation phases were fitted separately. The initial association process was fitted by linear regression to make possible a comparison of the incipient affinities of the proteins when inserting into the membrane directly and with a higher precision (as the initial slope is also proportional to $R_{max} - R(t)$ and c_P, only relative $k_{on,1}$ values can be compared by this means). The dissociation phase was fitted to a biexponential model (Eq. 4) as well, of which the average dissociation constant, $\overline{k}_{diss}$, was calculated (Eq. 5). This parameter is a measure of the overall dissociation rate of the proteins from the various membrane systems prepared. All kinetic data are presented as bar charts (Figs. 3–5), and all data from the two-step process are also summarized in Table S1 of the Supporting Material). Furthermore, we evaluated the relative amount of quasi-irreversibly bound protein at the end of each dissociation phase (Fig. 5 *C*).

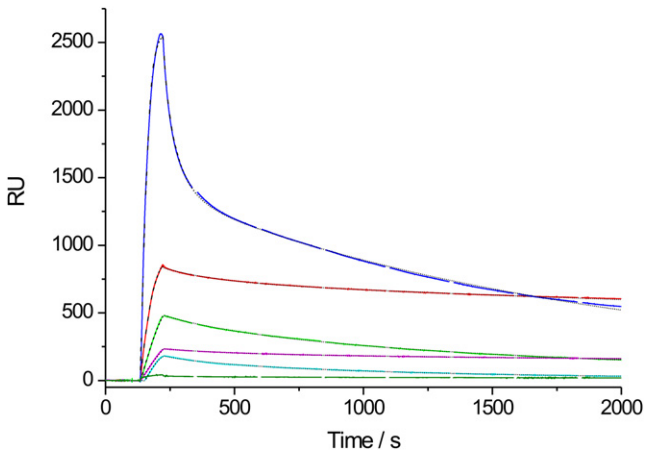

FIGURE 2 Sensorgrams of 1 μM N-Ras Far (*blue*), Far/Far (*red*), HD/HD (*turquoise*), HD/Far (GDP) (*pink*), HD/Far (GTP) (*green*), and nonlipidated N-Ras (*olive*) in the presence of a DOPC lipid bilayer. Respective fits to a two-step reaction model (Eqs. 2–4) are shown as dotted black lines. Sensorgrams were recorded at a frequency of 10 Hz.

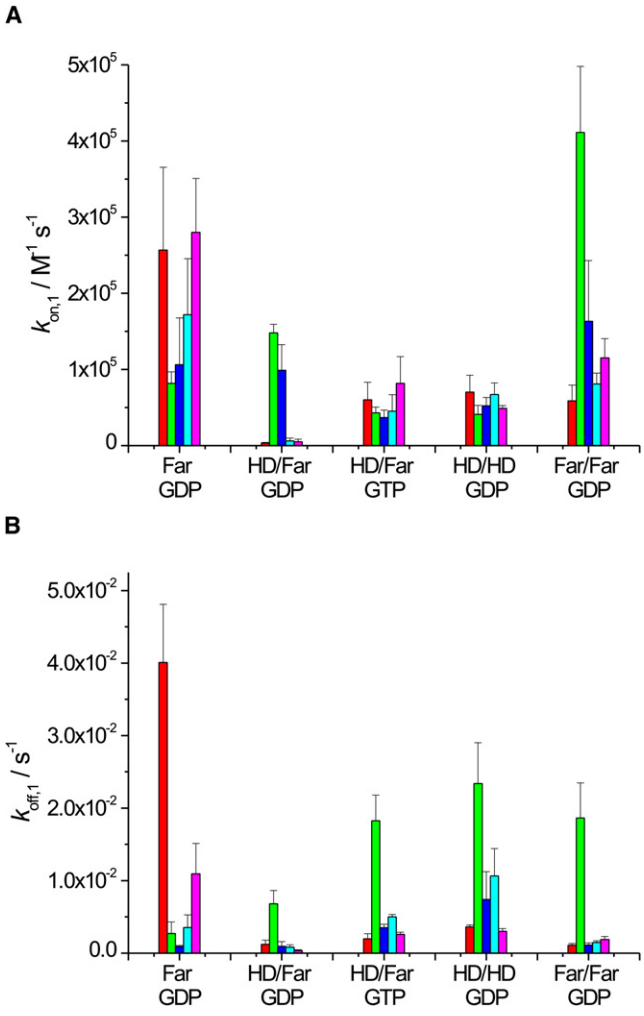

FIGURE 3 (*A*) $k_{on,1}$ and (B) $k_{off,1}$ values of N-Ras Far (GDP), HD/Far (GDP), HD/Far (GTP), HD/HD (GDP), and Far/Far (GDP) binding to a DOPC (*red*), DPPC/Chol (7:3) (*green*), DOPC/DPPC/Chol (1:2:1) (*blue*), DOPC/DOPG (7:3) (*turquoise*), or DOPC/DOPE (7:3) (*pink*) lipid bilayer. Values were derived from the SPR data by applying a two-step model fit. The error bars represent the standard deviation from at least three (up to six) independently conducted experiments.

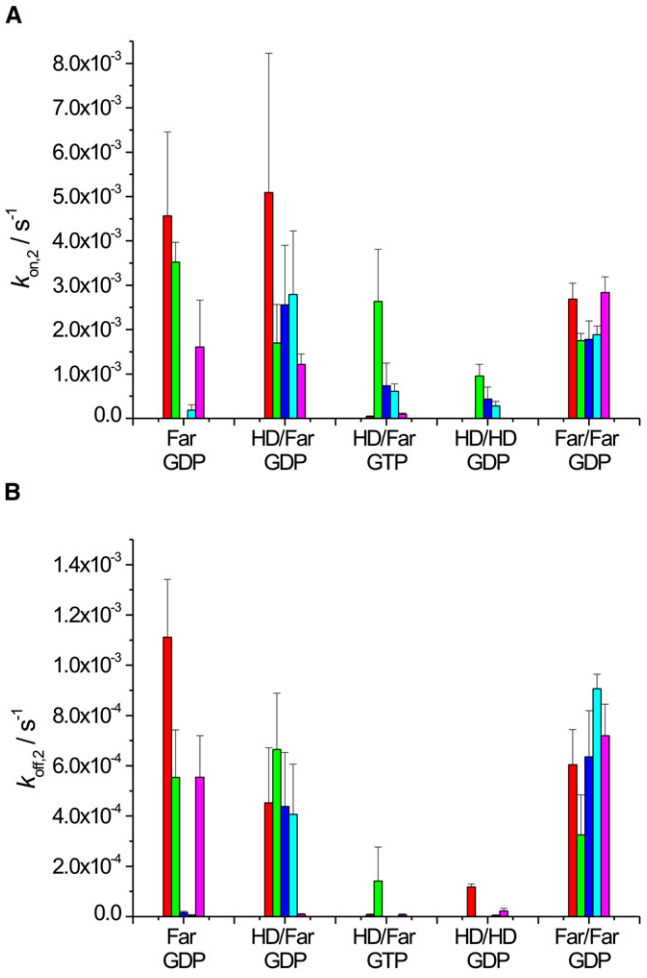

FIGURE 4 (*A*) $k_{on,2}$ and (*B*) $k_{off,2}$ values of N-Ras Far (GDP), HD/Far (GDP), HD/Far (GTP), HD/HD (GDP), and Far/Far (GDP) binding to a DOPC (*red*), DPPC/Chol (7:3) (*green*), DOPC/DPPC/Chol (1:2:1) (*blue*), DOPC/DOPG (7:3) (*turquoise*), or DOPC/DOPE (7:3) (*pink*) lipid bilayer. Values were derived from the SPR data by applying a two-step model fit. The error bars represent the standard deviation from at least three (up to six) independently conducted experiments.

The data for binding ($k_{on,1}$) of the N-Ras proteins to the various lipid bilayers (Fig. 3 *A*) show association rates on the order of 1–3 $\times$ 10^3–10^5 M^{-1} s^{-1}. Fastest association rates are observed for the monofarnesylated protein (N-Ras Far) in fluidlike bilayer environments, as already clearly visible in the primary data shown in Fig. 2. Slower binding is observed to a purely l_o phase (DPPC/Chol 7:3). The fast association of the monofarnesylated protein into the fluidlike membranes can be seen more clearly when evaluating the initial slopes of the sensorgrams (Fig. 5 *A*). Also, the doubly farnesylated form (Far/Far) exhibits a higher initial binding rate compared to the other doubly lipidated proteins, whereas insertion into the all-l_o phase is markedly retarded.

To cover also a heterogeneous membrane system, we measured the association and dissociation kinetics of the N-Ras constructs using a model raft mixture exhibiting $l_d + l_o$ phase coexistence, DOPC/DPPC/cholesterol (1:2:1).

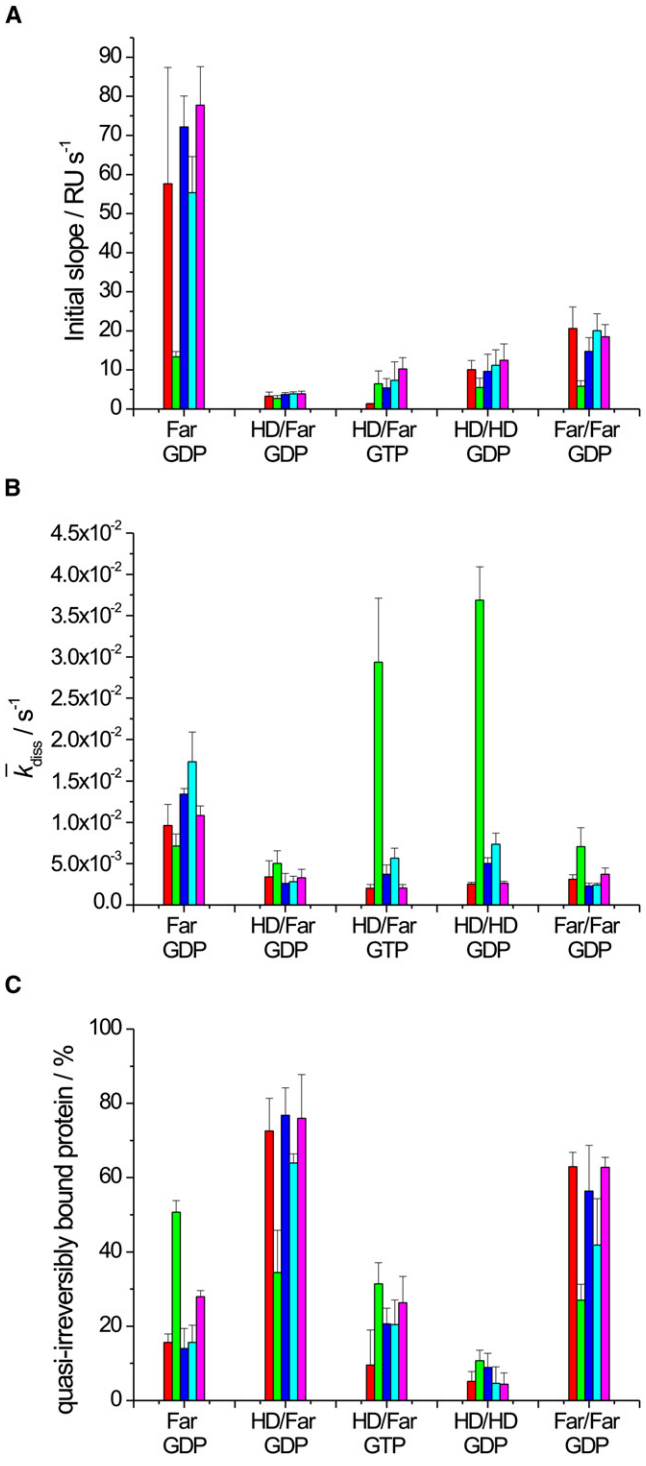

FIGURE 5 (*A*) Initial slope and (*B*) averaged dissociation constant of N-Ras Far (GDP), HD/Far (GDP), HD/Far (GTP), HD/HD (GDP), and Far/Far (GDP) binding to a DOPC (*red*), DPPC/Chol (7:3) (*green*), DOPC/DPPC/Chol (1:2:1) (*blue*), DOPC/DOPG (7:3) (*turquoise*), or DOPC/DOPE (7:3) (*pink*) lipid bilayer. (*C*) Corresponding relative amount of quasi-irreversibly bound protein. The error bars represent the standard deviation from at least three (up to six) independently conducted experiments.

It has already been reported that this ternary lipid mixture shows coexistence of the two phases at a temperature of 25°C (37). The initial slope of the association data (Fig. 5 *A*) for the model raft mixture is similar to that of all-fluidlike membranes, indicating that the N-Ras Far is partitioning into a fluidlike environment upon binding to the heterogeneous lipid bilayer.

Furthermore, the effect of lipid headgroup charge on the initial binding event was investigated. The N-Ras protein has a pI of 5.0 and therefore carries a net negative charge at a pH of 7.4. Hence, we wanted to explore to what extent electrostatic interactions influence the process of binding to the membrane. To this end, we prepared a lipid bilayer consisting of DOPC and DOPG in a molar ratio of 7:3, i.e., a bilayer membrane with a significant contribution of anionic lipids. As can be seen in Fig. 3 *A*, incorporation of anionic charges in the lipid headgroup region does not markedly change the initial binding event of N-Ras Far. This goes along with the evaluation of the initial SPR slope, where the binding of N-Ras to anionic lipids is found to be similar to the binding to the zwitterionic one (DOPC) (Fig. 5 *A*).

A large portion of the lipids encountered in natural membranes are type II lipids, which have a tendency toward interfacial curvature due to the nonuniform distribution of the lateral pressure between the amphiphiles. A useful way of quantifying the torque tension is in terms of the stored curvature elastic energy. For the type II lipid amphiphile DOPE, the stored curvature elastic energy for each DOPE molecule in a flat monolayer is ~1 k_BT. Incorporation of an amphipathic molecule, such as the membrane binding domain of a protein, allows the release of at least some of this stored curvature elastic energy. Hence, we may anticipate that the stored curvature elasticity may play a significant role in modulating the partitioning of peptides and other biomolecules into the membrane and hence in their function (38–40). Adding DOPE to DOPC vesicles increases the tendency for curvature toward the water because of the smaller size of the phosphatidylethanolamine headgroup. We tested the influence of stored curvature elastic stress on the binding properties of the lipidated N-Ras constructs by including 30% DOPE in a DOPC bilayer. As visible in Fig. 3 *A*, such an influence does not seem to play a marked role, though minor changes cannot be excluded. Within the experimental error, similar $k_{on,1}$ values, as well as initial association slopes (Fig. 5 *A*), were recorded.

As can be clearly seen in Figs. 3 *A* and 5 *A*, double lipidation leads to an overall decrease of the association process by a factor of 3–5, with average $k_{on,1}$ values of the order of 5×10^4 M^{-1} s^{-1}, less pronounced for the doubly farnesylated protein, however. Within the experimental error, no major differences are observed between the various fluid phases (whether zwitterionic, charged, or curvature-stressed), indicating that electrostatic interactions and stored curvature elastic energy have no major effect on the binding properties of the various lipidated proteins.

Calculation of the dissociation equilibrium constants of the initial binding event, $K_{D1} = k_{off,1}/k_{on,1}$, which may be evaluated assuming detailed balance and near-equilibrium conditions, reveals generally very small values on the order of $1–10 \times 10^{-8}$ M, with slightly higher values for N-Ras HD/Far (GTP) and HD/HD (GDP) in l_o membrane environments with values up to ~6×10^{-7} M, indicating rather stable association of the multiply lipidated protein. The single farnesylated protein and N-Ras HD/Far GDP show highest K_{D1} values in the l_d phase on the order of ~$1–4 \times 10^{-7}$ M.

The change in nucleotide loading (GTP versus GPD) of the natural N-Ras HD/Far does not lead to marked differences in the initial binding process of the lipidated protein. In general, in the case of the doubly lipidated proteins, the initial rate of binding to an l_o phase is of a similar order of magnitude.

The fast binding process of N-Ras Far to fluidlike membranes is mirrored in a comparatively fast dissociation process, as revealed in Fig. 3 *B*, where all $k_{off,1}$ data are shown. Generally, the $k_{off,1}$ values observed are on the order of $0.1–4 \times 10^{-2}$ s^{-1}, corresponding to halflives of the dissociation process from ~7×10^2 to 20 s. Fastest dissociation of the initial binding step in fluid bilayers is observed for N-Ras Far (Fig. 3 *B*) (for DOPC, $p < 0.0008$). The corresponding values for the double-anchor systems are smaller, reflecting more stable binding to the fluid bilayer membrane. Conversely, dissociation from an l_o membrane is more rapid, indicating less stable association of the doubly lipidated protein in bilayers of high conformational order ($p < 0.014$). It is interesting to note that the doubly hexadecylated form, N-Ras HD/HD (GDP), and the active form of N-Ras, N-Ras HD/Far (GTP), exhibit slightly larger dissociation rates, i.e., the GTP-loaded form of N-Ras HD/Far seems to dissociate more rapidly after initial binding compared to the inactive form, N-Ras HD/Far (GDP) ($p = 0.00121$). These findings are supported by the evaluation of the average overall dissociation rate (Fig. 5 *B*).

The initial binding process may be followed by a diffusion-controlled reorganization of the protein-lipid assembly within the lipid bilayer plane. Fig. 4 *A* depicts the corresponding $k_{on,2}$ values for this process, leading to a PL* state that might involve participation of nonlipid parts of the protein in the binding process and clustering within the various phases or, in the case of the heterogeneous model raft mixture, at the l_d/l_o domain boundaries to decrease the unfavorable line tension between coexisting domains. Recent AFM studies have shown that such a scenario should be taken into account as well (18). The $k_{on,2}$ values reveal rather slow reorganization processes, with rates mainly in the range of about $0.1–5 \times 10^{-3}$ s^{-1}. Such secondary association processes are observed for most systems, but with different time constants. Fastest formation of association clusters in fluid bilayers is observed for the monofarnesylated N-Ras, N-Ras HD/Far (GDP), and Far/Far (GDP). It is of interest that such a secondary kinetic process of

clustering seems to play a minor role for the active form of N-Ras, N-Ras HD/Far (GTP), and for the doubly hexadecylated form, N-Ras HD/HD (GDP), embedded in fluidlike membranes (see also below). In fact, recent time-lapse AFM studies have shown that N-Ras HD/HD has a very low propensity to aggregate even in heterogeneous raft mixtures. These AFM studies also reveal that diffusion and clustering at l_d/l_o domain boundaries of the model raft mixture DPPC/DOPC/Chol 1:2:1 is most pronounced for the farnesylated proteins (18).

Kinetically rather stable formation of PL* complexes is indicated by the very small dissociation rates, $k_{off,2}$, which are on the order of 3×10^{-7} to 1×10^{-3} s^{-1}. As might be expected from the lower binding energy of the farnesyl residue to lipid bilayers (41–43), fastest dissociation from the membrane platform—though still rather slow, i.e., on the order of several minutes—is observed for the monofarnesylated lipidated protein. Higher dissociation rates are also observed for N-Ras HD/Far (GDP) and N-Ras Far/Far (GDP). The overall equilibrium constant for the dissociation process, $K_D = (k_{off,1}/k_{on,1}) \times (k_{off,2}/k_{on,2})$, generally exhibits very small values, in the range 1–30 nM, with smallest values for the doubly lipidated peptides in the raft mixture, probably owing to extended clustering of the protein. Higher K_D values of ~10 μM are only observed for the N-Ras HD/HD embedded in fluid bilayers. For comparison, studies of lipidated model peptides revealed dissociation constants in the nanomolar to micromolar range as well (41).

The amount of quasi-irreversibly bound protein can also be estimated from the offset of the biexponential fit of the dissociation phase. As seen in Fig. 2, the offset values vary significantly with the lipidation motif. Fig. 5 *C* depicts the offset relative to the total amplitude of the dissociation phase at $t = 0$, which—at least qualitatively—reflects the ability of N-Ras to insert stably into the lipid bilayer system, eventually by forming stable protein assemblies upon association to the membrane. The data clearly reveal significant differences between the various lipidation motifs. Strong, quasi-irreversible binding is observed for N-Ras HD/Far (GDP) and Far/Far (GDP), in particular in fluidlike lipid environments (for DOPC, $p < 0.0022$). Marked differences are seen by changing the nucleotide loading of HD/Far. The GDP-bound form is more strongly bound, in particular in liquidlike environments, including the fluid domains of the model raft mixture (for DOPC, $p = 0.0053$). The doubly hexadecylated form of N-Ras exhibits the lowest amount of quasi-irreversibly bound protein (for DOPC in comparison to farnesylated GDP-loaded proteins, $p < 0.00033$). The nonlipidated form of N-Ras showed almost no binding to any of the membrane systems studied (Fig. 2).

DISCUSSION

Using SPR, we examined the association and dissociation behavior of various lipidated N-Ras constructs to model membranes comprising various kinds of physical-chemical characteristics. Significant differences were observed for the various anchor motifs. The non-simple-exponential association and dissociation curves reflect a complex interaction behavior for all systems studied. We evaluated the SPR data on the basis of a two-step model of protein-membrane interactions, which involves initial binding followed by insertion/dissociation of the protein into/from the hydrophobic interior of the membrane, as well as reorientation and potential clustering of the proteins in a secondary step. The protein sensorgrams typically did not return to zero with time, also indicating that a portion of the protein remains stably bound to the membrane. This amount of quasi-irreversibly bound protein might also be due to clustering of the proteins induced by lipid-mediated protein-protein interactions.

When evaluating the binding of N-Ras to the fluid DOPC bilayer exhibiting a pure l_d phase, it is obvious that the kind of lipid modification at the hypervariable region of N-Ras has a marked influence on the binding properties. In general, the monofarnesylated N-Ras (N-Ras Far) protein exhibits the highest association rate and fastest dissociation process (depending on the kind of fluidlike phase, on the order of several seconds up to a minute) when interacting with fluid-phase membranes. The amount of quasi-irreversibly bound protein induced by clustering followed by membrane insertion is rather low (~10–20%). Such behavior would be consistent with the weak membrane interaction proposed for monofarnesylated N-Ras and with the finding that N-Ras Far is easily displaced from the membrane for trafficking to the Golgi or ubiquitin-dependent degradation (7).

When comparing the (initial) association rate constants of N-Ras Far in the fluidlike phases with that in the all-l_o phase of DPPC/Chol (7:3), generally higher rates are found for the fluid phase. This behavior might be due to the strong hydrophobic mismatch between the hydrophobic length of the Far anchor and the all-*trans* C_{16} chain of ordered DPPC, as well as the bulky character of the farnesyl group. Generally, an increase of hydrophobic mismatch also is expected to drive clustering of proteins (44,45). Remarkably, it has been predicted that although transient, a dimer formation would still exist for an almost vanishing hydrophobic mismatch (45).

Double lipidation leads to an overall decrease of the association kinetics process in the fluid phase by a factor of ~5 (less pronounced for the doubly farnesylated protein, however). Double farnesylation also leads to a significant increase of protein self-assembly (~60%) in fluidlike phases (Fig. 5 *C*). Generally, dissociation from an l_o membrane is more rapid, indicating less stable binding of the doubly lipidated protein in bilayers of high conformational order (Figs. 3 *B* and 5 *B*).

In addition, we tested the influence of negative charges (by including 30 mol % negatively charged DOPG into the DOPC bilayer) on the binding properties of the lipidated N-Ras proteins. The typical amount of charges, mainly

located at the inner leaflet of the plasma membrane, is <~20% (46–48). Here, we conducted experiments with bilayers comprised of 30% anionic lipids to probe the maximum charge effect. For the doubly lipidated proteins, the association and dissociation processes, as well as the relative contributions of strongly bound protein, are similar to those of the pure DOPC bilayer.

Furthermore, the inclusion of 30% DOPE into the DOPC bilayer hardly showed any effect on the association and dissociation process of the N-Ras proteins when compared to the purely fluid zwitterionic DOPC bilayer. Addition of DOPE increases the stored curvature elastic stress and it is known that in some cases the release of this stress by insertion of membrane-associated proteins can be a driving force for insertion into the membrane and sorting of the protein within the membrane (39,40). Phosphatidylethanolamines are also enriched in the inner leaflet of the plasma membrane by up to ~30% (46–48). As no marked effect is observed here, we may conclude that there is no significant contribution of curvature elastic stress to the behavior of binding of the lipidated N-Ras proteins to the membrane. This would be in agreement with the notion that the N-Ras protein inserts into the bilayer essentially with its acyl chains only, i.e., it is essentially driven by hydrophobic interactions with the acyl chains of the lipid bilayer systems, and the binding of the protein core does not play a major role.

To support the hypothesis that the N-Ras isoforms bind to the l_d phase rather than to the l_o phase, we also measured the binding of the N-Ras proteins to a heterogeneous DOPC/DPPC/Chol (1:2:1) bilayer showing coexistence of l_o and l_d domains, i.e., a canonical model raft mixture. Comparing the initial k_{on} and average k_{off} values, we found that the binding behavior mimics the binding to the pure l_d phase more than to the l_o phase (Fig. 5). Minor differences are expected, as the fluid phase in the raft mixture is more ordered due to the presence of saturated phospholipid and cholesterol (49). The preference of lipidated N-Ras to insert into the fluid rather than the ordered domains has also been shown in earlier fluorescence microscopy studies on giant unilamellar vesicles using an N-Ras peptide (22), as well as on the full-length lipidated protein (50).

The change in nucleotide loading (GTP versus GDP) for the natural N-Ras HD/Far does lead to minor differences in the initial binding process of the lipidated protein only. The active form of N-Ras, N-Ras HD/Far (GTP), exhibits slightly larger dissociation rates compared to the inactive, GDP-loaded form in the l_o phase (Figs. 3 *B* and 5 *B*). The amount of strongly bound protein is significantly higher in N-Ras HD/Far (GDP) (~70%) than in HD/Far (GTP) (~20%), most likely due to stronger intermolecular lipid-mediated protein-protein interactions (clustering) and/or an additional significant binding contribution by the HVR of the protein induced by conformational changes of the protein in the switch regions. The nonlipid side chains of the HVR of the protein might contribute to the binding affinity and/or cluster formation in step 2 after insertion is achieved. In fact, it has been suggested by molecular dynamics simulations on H-Ras that changes in the switch regions influence the orientation of the protein bound to the lipid interface (8). In the case of H-Ras, it has been found that the membrane interaction is mainly supported by distinct amino acids in the HVR and the helix $\alpha 4$, whose orientation toward the membrane is changed upon activation. This results in a different way of interacting with the membrane (8) and might also lead to changes in intermolecular interactions of the membrane-bound proteins. Moreover, it has been described that H-Ras in its monopalmitoylated form at Cys^{181} mimics the GTP-regulated membrane microdomain interactions of N-Ras (17).

Remarkably, the doubly hexadecylated N-Ras protein shows a comparatively low tendency for stable membrane insertion despite similar association rates (Fig. 5). This behavior is probably due to the highly flexible nature of the two hexadecyl chains. Their insertion requires a costly decrease of conformational entropy, in particular in cases with marked hydrophobic mismatch between the lipid bilayer and the lipid anchors of the protein. Such high flexibility would be in accord with recent findings from ^{2}H-NMR data (21,50).

To conclude, we have determined that the natural N-Ras Far protein inserts rapidly and preferentially into a fluidlike lipid bilayer environment rather than a rigid, ordered environment. Double lipidation, such as in the natural N-Ras HD/Far, leads to drastically reduced initial binding rates but stronger association (Fig. 5, *A* and *C*), and the average dissociation process from fluidlike environments is retarded as well (Fig. 5 *B*). This is in agreement with previous findings that singly farnesylated model peptides are kinetically more unstable in the membrane than the HD/Far isoform of N-Ras, with halflives of a few seconds compared to several minutes for the initial binding process (41). It has also been reported that depalmitoylation of N-Ras is necessary for retrograde trafficking of N-Ras from the plasma membrane to the Golgi (7). Comparison with such model peptide studies must be made with care, however, as shown, for example, by experimental work on the hedgehog protein (51) and by molecular dynamics simulations (8) on H-Ras in DMPC bilayers, showing that the protein corpus and also the GTP versus GDP loading may have some influence on the partitioning behavior and adsorption kinetics, and hence probably also on lipid-mediated protein-protein interactions and clustering. The inclusion of charges or negative curvature elastic stress does not seem to have a drastic influence on the association and dissociation kinetics, although minor effects cannot be excluded. A change in nucleotide loading of N-Ras HD/Far induces a slightly different association and dissociation kinetics, as well as stability of binding, and might help regulate the tendency to segregate laterally in the membrane plane. The natural inactive form of N-Ras, N-Ras HD/Far (GDP), shows stronger quasi-irreversible

binding, which might be due to its higher tendency to self-assemble in the membrane matrix compared to the active form, N-Ras HD/Far (GTP). Generally, protein clusters are expected to have longer lifetimes and might play an important role in the biological context of signaling, which involves interaction with membrane-associated effectors and regulators. In the kinetically trapped state, the protein will dissociate from the membrane with extremely slow kinetics unless the process is accelerated by specific cellular factors, such as membrane-bound scaffolding or regulatory proteins. Hence, addition of membrane-associated effector molecules, as, for example, Sos or galectins, may be expected to interact with N-Ras HD/Far (GTP) and HD/Far (GDP) in different ways.

SUPPORTING MATERIAL

One table is available at http://www.biophysj.org/biophysj/supplemental/S0006-3495(10)00233-X.

Financial support from the Deutsche Forschungsgemeinschaft (SFB 642) is gratefully acknowledged.

REFERENCES

1. Karnoub, A. E., and R. A. Weinberg. 2008. Ras oncogenes: split personalities. *Nat. Rev. Mol. Cell Biol.* 9:517–531.
2. Bos, J. L. 1989. Ras oncogenes in human cancer: a review. *Cancer Res.* 49:4682–4689.
3. Wittinghofer, A., and H. Waldmann. 2000. Ras: a molecular switch involved in tumor formation. *Angew. Chem. Int. Ed.* 39:4192–4214.
4. Omerovic, J., D. E. Hammond, …, I. A. Prior. 2008. Ras isoform abundance and signalling in human cancer cell lines. *Oncogene.* 27:2754–2762.
5. Hancock, J. F., and R. G. Parton. 2005. Ras plasma membrane signalling platforms. *Biochem. J.* 389:1–11.
6. Goodwin, J. S., K. R. Drake, …, A. K. Kenworthy. 2005. Depalmitoylated Ras traffics to and from the Golgi complex via a nonvesicular pathway. *J. Cell Biol.* 170:261–272.
7. Rocks, O., A. Peyker, …, P. I. Bastiaens. 2005. An acylation cycle regulates localization and activity of palmitoylated Ras isoforms. *Science.* 307:1746–1752.
8. Abankwa, D., A. A. Gorfe, and J. F. Hancock. 2007. Ras nanoclusters: molecular structure and assembly. *Semin. Cell Dev. Biol.* 18:599–607.
9. Hancock, J. F. 2006. Lipid rafts: contentious only from simplistic standpoints. *Nat. Rev. Mol. Cell Biol.* 7:456–462.
10. Laude, A. J., and I. A. Prior. 2004. Plasma membrane microdomains: organization, function and trafficking. *Mol. Membr. Biol.* 21: 193–205.
11. Lobo, S., W. K. Greentree, …, R. J. Deschenes. 2002. Identification of a Ras palmitoyltransferase in *Saccharomyces cerevisiae*. *J. Biol. Chem.* 277:41268–41273.
12. Pechlivanis, M., R. Ringel, …, J. Kuhlmann. 2007. Prenylation of Ras facilitates hSOS1-promoted nucleotide exchange, upon Ras binding to the regulatory site. *Biochemistry.* 46:5341–5348.
13. Silvius, J. R. 2005. Partitioning of membrane molecules between raft and non-raft domains: insights from model-membrane studies. *Biochim. Biophys. Acta.* 1746:193–202.
14. Simons, K., and D. Toomre. 2000. Lipid rafts and signal transduction. *Nat. Rev. Mol. Cell Biol.* 1:31–39.
15. Zacharias, D. A., J. D. Violin, …, R. Y. Tsien. 2002. Partitioning of lipid-modified monomeric GFPs into membrane microdomains of live cells. *Science.* 296:913–916.
16. Zhao, L., S. Lobo, …, R. J. Deschenes. 2002. Erf4p and Erf2p form an endoplasmic reticulum-associated complex involved in the plasma membrane localization of yeast Ras proteins. *J. Biol. Chem.* 277:49352–49359.
17. Roy, S., S. Plowman, …, J. F. Hancock. 2005. Individual palmitoyl residues serve distinct roles in H-ras trafficking, microlocalization, and signaling. *Mol. Cell. Biol.* 25:6722–6733.
18. Weise, K., G. Triola, …, R. Winter. 2009. Influence of the lipidation motif on the partitioning and association of N-Ras in model membrane subdomains. *J. Am. Chem. Soc.* 131:1557–1564.
19. Rajendran, L., and K. Simons. 2005. Lipid rafts and membrane dynamics. *J. Cell Sci.* 118:1099–1102.
20. Reuther, G., K. T. Tan, …, D. Huster. 2006. Structural model of the membrane-bound C terminus of lipid-modified human N-ras protein. *Angew. Chem. Int. Ed.* 45:5387–5390.
21. Reuther, G., K. T. Tan, …, D. Huster. 2006. The lipidated membrane anchor of full length N-Ras protein shows an extensive dynamics as revealed by solid-state NMR spectroscopy. *J. Am. Chem. Soc.* 128:13840–13846.
22. Janosch, S., C. Nicolini, …, R. Winter. 2004. Partitioning of dual-lipidated peptides into membrane microdomains: lipid sorting vs peptide aggregation. *J. Am. Chem. Soc.* 126:7496–7503.
23. Meister, A., C. Nicolini, …, A. Blume. 2006. Insertion of lipidated Ras proteins into lipid monolayers studied by infrared reflection absorption spectroscopy (IRRAS). *Biophys. J.* 91:1388–1401.
24. Bader, B., K. Kuhn, …, J. Kuhlmann. 2000. Bioorganic synthesis of lipid-modified proteins for the study of signal transduction. *Nature.* 403:223–226.
25. Brunsveld, L., J. Kuhlmann, …, H. Waldmann. 2006. Lipidated Ras and Rab peptides and proteins: synthesis, structure, and function. *Angew. Chem. Int. Ed.* 45:6622–6646.
26. Kragol, G., M. Lumbierres, …, H. Waldmann. 2004. Solid-phase synthesis of lipidated peptides. *Angew. Chem. Int. Ed.* 43:5839–5842.
27. Nägele, E., M. Schelhaas, …, H. Waldmann. 1998. Chemoenzymatic synthesis of N-Ras lipopeptides. *J. Am. Chem. Soc.* 120:6889–6902.
28. Reents, R., M. Wagner, …, H. Waldmann. 2004. Synthesis and application of fluorescence-labeled Ras-proteins for live-cell imaging. *Angew. Chem. Int. Ed.* 43:2711–2714.
29. Schelhaas, M., S. Glomsda, …, H. Waldmann. 1996. Enzymatische Synthese von Peptiden und Ras-Lipopeptiden unter Verwendung des Cholinesters als löslichkeitsvermittelnder Schutz- und Aktivierungsgruppe. *Angew. Chem.* 35:106–109.
30. Waldmann, H., and E. Nägele. 1995. Synthesis of the palmitoylated and farnesylated C-terminal lipohexapeptide of the human N-Ras protein by employing an enzymatically removable urethane protecting group. *Angew. Chem. Int. Ed. Engl.* 34:2259–2262.
31. Lenzen, C., R. H. Cool, …, A. Wittinghofer. 1998. Kinetic analysis by fluorescence of the interaction between Ras and the catalytic domain of the guanine nucleotide exchange factor Cdc25Mm. *Biochemistry.* 37:7420–7430.
32. Lenzen, C., R. H. Cool, and A. Wittinghofer. 1995. Analysis of intrinsic and CDC25-stimulated guanine nucleotide exchange of p21ras-nucleotide complexes by fluorescence measurements. *Methods Enzymol.* 255:95–109.
33. Mayer, L. D., M. J. Hope, and P. R. Cullis. 1986. Vesicles of variable sizes produced by a rapid extrusion procedure. *Biochim. Biophys. Acta.* 858:161–168.
34. Mozsolits, H., W. G. Thomas, and M. I. Aguilar. 2003. Surface plasmon resonance spectroscopy in the study of membrane-mediated cell signalling. *J. Pept. Sci.* 9:77–89.
35. Besenicar, M., P. Macek, …, G. Anderluh. 2006. Surface plasmon resonance in protein-membrane interactions. *Chem. Phys. Lipids.* 141: 169–178.

36. Vist, M. R., and J. H. Davis. 1990. Phase equilibria of cholesterol/dipalmitoylphosphatidylcholine mixtures: ^{2}H nuclear magnetic resonance and differential scanning calorimetry. *Biochemistry*. 29:451–464.

37. Jeworrek, C., M. Pühse, and R. Winter. 2008. X-ray kinematography of phase transformations of three-component lipid mixtures: a time-resolved synchrotron x-ray scattering study using the pressure-jump relaxation technique. *Langmuir*. 24:11851–11859.

38. Attard, G. S., R. H. Templer, …, S. Jackowski. 2000. Modulation of CTP:phosphocholine cytidylyltransferase by membrane curvature elastic stress. *Proc. Natl. Acad. Sci. USA*. 97:9032–9036.

39. Ces, O., and X. Mulet. 2006. Physical coupling between lipids and proteins: a paradigm for cellular control. *Signal Transduct.* 6:112–132.

40. Sorre, B., A. Callan-Jones, …, P. Bassereau. 2009. Curvature-driven lipid sorting needs proximity to a demixing point and is aided by proteins. *Proc. Natl. Acad. Sci. USA*. 106:5622–5626.

41. Silvius, J. R., and F. l'Heureux. 1994. Fluorimetric evaluation of the affinities of isoprenylated peptides for lipid bilayers. *Biochemistry*. 33:3014–3022.

42. Wang, T.-Y., R. Leventis, and J. R. Silvius. 2000. Fluorescence-based evaluation of the partitioning of lipids and lipidated peptides into liquid-ordered lipid microdomains: a model for molecular partitioning into "lipid rafts". *Biophys. J*. 79:919–933.

43. Brunsveld, L., H. Waldmann, and D. Huster. 2009. Membrane binding of lipidated Ras peptides and proteins—the structural point of view. *Biochim. Biophys. Acta*. 1788:273–288.

44. Jensen, M. O., and O. G. Mouritsen. 2004. Lipids do influence protein function-the hydrophobic matching hypothesis revisited. *Biochim. Biophys. Acta*. 1666:205–226.

45. Schmidt, U., G. Guigas, and M. Weiss. 2008. Cluster formation of transmembrane proteins due to hydrophobic mismatching. *Phys. Rev. Lett.* 101:128104.

46. Devaux, P. F., and R. Morris. 2004. Transmembrane asymmetry and lateral domains in biological membranes. *Traffic*. 5:241–246.

47. Rothman, J. E., and J. Lenard. 1977. Membrane asymmetry. *Science*. 195:743–753.

48. van Meer, G., D. R. Voelker, and G. W. Feigenson. 2008. Membrane lipids: where they are and how they behave. *Nat. Rev. Mol. Cell Biol.* 9:112–124.

49. Nicolini, C., J. Kraineva, …, R. Winter. 2006. Temperature and pressure effects on structural and conformational properties of POPC/SM/cholesterol model raft mixtures—a FT-IR, SAXS, DSC, PPC and Laurdan fluorescence spectroscopy study. *Biochim. Biophys. Acta*. 1758:248–258.

50. Vogel, A., G. Reuther, …, D. Huster. 2009. The lipid modifications of Ras that sense membrane environments and induce local enrichment. *Angew. Chem. Int. Ed.* 48:8784–8787.

51. Peters, C., A. Wolf, …, H. Waldmann. 2004. The cholesterol membrane anchor of the hedgehog protein confers stable membrane association to lipid-modified proteins. *Proc. Natl. Acad. Sci. USA*. 101:8531–8536.